IEEE Access
Multidisciplinary | Rapid Review | Open Access Journal

Received January 17, 2020, accepted February 9, 2020, date of publication February 19, 2020, date of current version March 2, 2020.

Digital Object Identifier 10.1109/ACCESS.2020.2975087

An Accuracy Enhancement Method for a Cable-Driven Continuum Robot With a Flexible Backbone

WENJUN SHEN[1,2], GUILIN YANG[1], (Member, IEEE), TIANJIANG ZHENG[1], YI WANG[1,2], KAISHENG YANG[1,2,3], AND ZAOJUN FANG[1]

[1]Zhejiang Key Laboratory of Robotics and Intelligent Manufacturing Equipment Technology, Ningbo Institute of Materials Technology and Engineering, Chinese Academy of Sciences, Ningbo 315201, China
[2]University of Chinese Academy of Sciences, Beijing 100049, China
[3]Zhejiang Marine Development Research Institute, Zhoushan 316021, China

Corresponding author: Guilin Yang (glyang@nimte.ac.cn)

This work was supported in part by the National Natural Science Foundation of China under Project 51705510, in part by the NSFC-Zhejiang Joint Found for the Integration and Information under Project U1509202 and Project U1909215, and in part by the Institute of Robotics and Intelligent Manufacturing Innovation, Chinese Academy of Sciences, under Project C2018005.

ABSTRACT In this paper, an integrated accuracy enhancement method based on both the kinematic model and the data-driven Gaussian Process Regression (GPR) technique is proposed for a Cable-Driven Continuum Robot (CDCR) with a flexible backbone. Different from the conventional continuum robots driven by pneumatic actuators, a segmented CDCR is developed in this work, which is a modular manipulator composed by a number of consecutive Cable-Driven Segments (CDSs). Based on the unique design of the backbone structure which merely allows 2-DOF bending motions, a two-variable Product-of-Exponential (POE) formula is employed to formulate the kinematic model of the CDCR. However, such an analytic kinematic model is unable to accurately describe the actual deflections of the backbone structure. Therefore, GPR is proposed to compensate the tip error of a CDCR. Compared with other machine learning methods, GPR requires less learning parameters and training data, which makes the learning process computationally efficient. To validate the effectiveness of the proposed integrated accuracy enhancement method, experiments on the actual testbed are conducted. Experimental results show that the CDCR's position and orientation errors are reduced by 68.72% and 51.74%, respectively.

INDEX TERMS Cable-driven continuum robot, kinematic modeling, tip error compensation, Gaussian process regression.

I. INTRODUCTION

A Cable-Driven Continuum Robot (CDCR) with a flexible backbone can realize continuous deformation in order to adapt to congested and complex environments. Besides, the CDCR has the advantages of light-weight structure, high compliance and inherent safety. Therefore, the CDCR has attracted many researchers' attention due to its promising applications, such as light-weight manipulators [1], [2], inspection of gas turbine engines [3] and minimally invasive surgery [4], [5].

In recent years, a variety of continuum robots have been developed for different working environments. In [6], a continuum soft robot is developed inspired by the octopus. The integral structure of the robot arm is made of silicone rubber, in which the driving cables are embedded into the structure. The proposed continuum robot possesses the bending, elongation and shrinking capabilities. In [7], a soft modular manipulator is presented based on flexible fluidic actuators and motor driven cables, which also allows bending, elongation and shrinking movements. In [8], a tendril robot driven by cables is proposed whose backbone employs extension and compression springs, and such a vimineous robot arm is employed for minimally invasive inspection. The above soft continuum robots have unique configuration designs in order to satisfy the properties such as high compliance, great environmental suitability and multi-degrees-of-freedom movements. However, due to the complex deformation of the

The associate editor coordinating the review of this manuscript and approving it for publication was Rui-Jun Yan.

This work is licensed under a Creative Commons Attribution 4.0 License. For more information, see http://creativecommons.org/licenses/by/4.0/

robot arm, it is difficult to formulate an accurate kinematic model.

In previous research, a variety of kinematic modeling methods have been proposed for different configuration designs of the flexible continuum robots. In [9], the conventional D-H parameter method is employed for the kinematic modeling analysis of a continuum robot inspired by the elephant trunk. In [10], the forward kinematic model of a multi-backbone snake-like robot is formulated based on a two-joint-variable formula, in which two joint variables are employed to describe the bending movements of the backbone. In [11], a modal analysis approach is proposed to develop the kinematic model of a hyper-redundant continuum robot. The shape of the flexible backbone is decomposed into a finite number of Wavelet basis functions in order to approximate the actual bending shape of the backbone. However, as most continuum robots have complex deformation due to their soft and flexible backbone structures, their kinematic models formulated through the above modeling methods are generally inaccurate, which significantly affect the positioning accuracy of the continuum robots.

In order to improve the accuracy of the kinematic model, various machine learning methods are employed for flexible continuum robots. In [12], a supervised learning method, Feedforward Neural Network (FNN), is employed to learn the inverse kinematic model for an nonconstant curvature soft manipulator. Compared with the numerical inverse kinematics algorithm, the presented method shows good performance and significantly compensates the position error. In [13], three data-driven approaches, Extreme Learning Machine (ELM), Gaussian Mixture Regression (GMR) and K-Nearest Neighbors Regression (KNNR), are employed to learn the inverse kinematic model for a tendon-driven surgical manipulator to compensate its tip error. In [14], the forward and inverse kinematic models are obtained based on FNN technique for a concentric tube continuum robot, which shows good performance on the compensation of the translation and rotation errors. Compared with the analytic kinematic modeling approaches, the above data-based methods can effectively obtain more accurate kinematic models for flexible continuum robots. However, most machine learning methods require a large amount of training data and many learning parameters, which makes the learning process computationally intensive. Furthermore, the over-fitting problem in some machine learning methods also affects the accuracy of the learning models.

In this paper, a CDCR with a flexible backbone is designed, in which a segmented cable-driven scheme is employed. The flexible backbone employs a unique mechanical structure that has high tensile and torsional stiffness but low bending stiffness, so that each Cable-Driven Segment (CDS) merely allows 2-DOF bending movements. Such a backbone structure design not only simplifies the kinematic modeling process but also makes the resultant kinematic model more accurate than other continuum robots. Based on the unique design features, a two-variable POE formula [15], [16] is employed to formulate the forward kinematic model for the CDCR. However, there still exists the certain level of modeling errors due to the complex bending deflection of the backbone. Therefore, Gaussian Process Regression (GPR) technique is employed to compensate the tip error of the CDCR resulting from the analytic kinematic model, which further improves the accuracy of the kinematic model. The proposed method is integrated with the analytic kinematic model compared with other data-based machine learning methods. It requires less training parameters and training data, which increases the computational efficiency of the learning process.

The remainder of this paper is organized as follows: Section II presents the design of the CDCR with a unique flexible backbone structure. Section III presents the forward kinematic modeling analysis for the 2-DOF CDS and the CDCR, respectively. Section IV introduces GPR and the learning process in order to compensate the tip error of the CDCR. Section V presents the experimental set-up and experimental results to validate the effectiveness of the proposed integrated accuracy enhancement method. Finally, Section VI presents the conclusion of this work.

II. DESIGN FOR THE CABLE-DRIVEN CONTINUUM ROBOT WITH A FLEXIBLE BACKBONE

In this work, a segmented cable-driven scheme is employed for the CDCR with a flexible backbone. As shown in Fig.1a, the CDCR consists of a succession of consecutive identical Cable-Driven Segments (CDSs). Each CDS is independently controlled by four driving cables. The flexible backbone employs a wire braided hydraulic hose, which has low bending stiffness but high tensile and torsional stiffness. As a result of such a unique backbone design, the bending deflection of each CDS can be approximated by an arc, i.e., each CDS merely allows 2-DOF bending movements.

Referring to Fig.1b, each 2-DOF CDS consists of a base, a moving platform, four driving cables and a flexible backbone. For each CDS, the base is identical to the moving

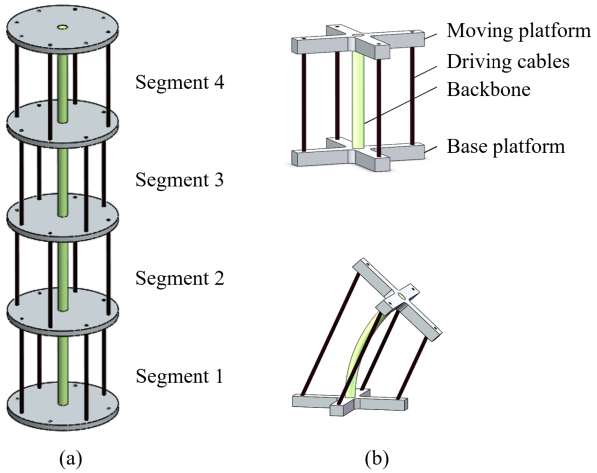

FIGURE 1. Schematic diagrams. a) The complete CDCR; b) the 2-DOF CDS.

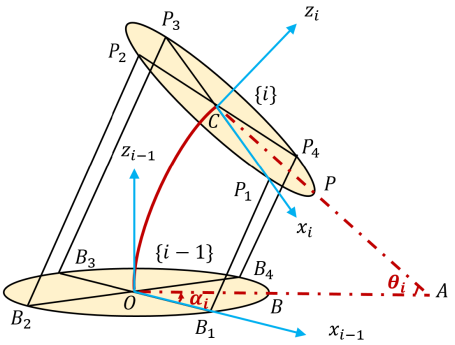

FIGURE 2. Kinematics diagram of the 2-DOF CDS.

platform. Four driving cables, which possess the unilateral driving property, are evenly anchored on both the base and the moving platform. The flexible backbone is located at the centers of the base and the moving platform.

Resulting from the unique flexible backbone structure, the kinematic modeling analysis of the CDCR is greatly simplified compared with other continuum robots which have complex movements.

III. FORWARD KINEMATIC MODELING ANALYSIS

A. FORWARD KINEMATIC MODELING ANALYSIS OF ONE CABLE-DRIVEN SEGMENT

As shown in Fig.2, for the i^{th} CDS, two coordinate systems, frame $\{i-1\}$ and frame $\{i\}$, are defined and located at the centers of the base and the moving platform, respectively. For frame $\{i-1\}$, its x_{i-1} axis points to the anchorage point of the first driving cable on the base and z_{i-1} axis is perpendicular to the base. Similarly, for frame $\{i\}$, its x_i axis points to the anchorage point of the first driving cable on the moving platform and z_i axis is perpendicular to the moving platform. The pose of the moving platform described in the base frame is represented by the kinematic transformation matrix from frame $\{i-1\}$ to frame $\{i\}$.

Based on the 2-DOF bending property, two joint variables are employed to describe the 2-DOF bending movements of the CDS: the bending angle θ_i and the rotation angle of the bending plane α_i, where $\theta_i \in [0, \frac{\pi}{2}]$, $\alpha_i \in [-\pi, \pi]$. The plane $OCPB$ presented in Fig.2 is the bending plane of the CDS, which is always perpendicular to the base.

1) KINEMATIC RELATIONSHIP BETWEEN DRIVING CABLE LENGTHS AND TWO JOINT VARIABLES

Define the norm of the vector $\overrightarrow{B_jP_j}$ be the j^{th} driving cable length ($j = 1, 2, 3, 4$). Based on the kinematics diagram referring to Fig.2, a close-loop equation for the $\overrightarrow{B_jP_j}$ is given as

$$\overrightarrow{B_jP_j} = \overrightarrow{B_jO} + \overrightarrow{OC} + \overrightarrow{CP_j} \tag{1}$$

where B_j and P_j denote the anchorage points of the j^{th} driving cable on the base and the moving platform, respectively. O and C are the central points of the base and the moving platform, respectively. The vectors, $\overrightarrow{B_jO}$, $\overrightarrow{OC}$ and $\overrightarrow{CP_j}$, can be formulated by the joint variables and geometric parameters of the CDS.

According to (1), the analytic expression of the j^{th} driving cable length is formulated as

$$l_{ij} = 2\frac{L}{\theta_i}\sin\frac{\theta_i}{2} - 2r\cos\beta_j\sin\frac{\theta_i}{2} \tag{2}$$

where L is the arc length of the backbone, and r is the radius of the circle where the anchorage points are located.

In (2), β_j is the rotation angle from $\overrightarrow{OB_j}$ to $\overrightarrow{OB}$. It can be expressed as

$$\beta_j = \alpha + (j-1)\frac{\pi}{2} \tag{3}$$

where $j = 1, 2, 3, 4$.

From (2), it yields

$$\alpha_i = \arctan\left(\frac{l_{i4} - l_{i2}}{l_{i3} - l_{i1}}\right) \tag{4}$$

$$\theta_i = 2\arcsin\left(\frac{\sqrt{(l_{i3} - l_{i1})^2 + (l_{i4} - l_{i2})^2}}{4r}\right) \tag{5}$$

According to (4) and (5), the kinematic relationship between driving cable lengths and two joint variables is clearly expressed.

2) KINEMATIC RELATIONSHIP BETWEEN TWO JOINT VARIABLES AND THE POSE OF THE MOVING PLATFORM

Based on the screw theory, the 2-DOF bending motions of the CDS can be described as the rotation about an instantaneous screw axis ξ_i by the bending angle θ_i [17]. The kinematic transformation matrix of frame $\{i\}$ with respect to frame $\{i-1\}$ is given as

$$T_{i-1,i}(\alpha_i, \theta_i) = e^{\hat{\xi}_i\theta_i}T_{i-1,i}(0) \tag{6}$$

where $\hat{\xi}_i = \begin{bmatrix} \hat{\omega}_i & v_i \\ 0 & 0 \end{bmatrix} \in se(3)$ is the twist of the i^{th} CDS described in frame $\{i-1\}$, whose twist coordinate is given by the screw axis $\xi_i = (v_i, \omega_i) \in \Re^{6\times1}$. v_i represents the position vector of the screw axis ξ_i described in frame $\{i-1\}$ and ω_i is the unit directional vector of the screw axis ξ_i described in frame $\{i-1\}$.

In (6), $T_{i-1,i}(0)$ denotes the initial pose of frame $\{i\}$ expressed in frame $\{i-1\}$:

$$T_{i-1,i}(0) = \begin{bmatrix} 1 & 0 & 0 & 0 \\ 0 & 1 & 0 & 0 \\ 0 & 0 & 1 & L \\ 0 & 0 & 0 & 1 \end{bmatrix} \tag{7}$$

To determine $\xi_i = (v_i, \omega_i) \in \Re^{6\times1}$, the kinematic transformation from frame $\{i-1\}$ to frame $\{i\}$ is employed:

$$T_{i-1,i}(\alpha_i, \theta_i) = \begin{bmatrix} R_{i-1,i}(\alpha_i, \theta_i) & p(\alpha_i, \theta_i) \\ 0 & 1 \end{bmatrix} \tag{8}$$

where $R_{i-1,i}(\alpha_i, \theta_i) = e^{\hat{\omega}_i\theta_i} \in SO(3)$ is the orientation of frame $\{i\}$ with respect to frame $\{i-1\}$, and $p(\alpha_i, \theta_i)$ is the

position vector of frame $\{i\}$ with respect to frame $\{i-1\}$, which is represented by the coordinate of $\overrightarrow{OC}$.

According to (6) and (8), $e^{\hat{\xi}_i\theta_i}$ can be rewritten as

$$e^{\hat{\xi}_i\theta_i} = T_{i-1,i}(\alpha_i, \theta_i)T_{i-1,i}(0)^{-1} \tag{9}$$

From [17], the twist motion $e^{\hat{\xi}_i\theta_i}$ can also be represented as

$$e^{\hat{\xi}_i\theta_i} = \begin{bmatrix} e^{\hat{\omega}_i\theta_i} & (I - e^{\hat{\omega}_i\theta_i})(\omega_i \times v_i) + \omega_i\omega_i^T v_i\theta_i \\ 0 & 1 \end{bmatrix} \tag{10}$$

Through equating (9) and (10), the position and orientation of the screw axis can be formulated as follows:

$$v_i = L\left[-\tfrac{1}{2}\cos\alpha_i \ -\tfrac{1}{2}\sin\alpha_i \ \tfrac{1}{\theta_i} - \tfrac{1}{2}\cot\tfrac{1}{\theta_i}\right]^T \tag{11}$$

$$\omega_i = \left[-\sin\alpha_i \ \cos\alpha_i \ 0\right]^T \tag{12}$$

According to (12), the orientation of the screw axis ω_i is consistently parallel to the base platform as shown in Fig.3. It is formed by the cross product of z_{i-1} and z_i and is perpendicular to the bending plane.

Based on (11) and (12), given two joint variables, α_i and θ_i, the screw axis can be uniquely determined. According to (6), the pose of the moving platform with respect to the base can be readily determined.

B. FORWARD KINEMATIC MODELING ANALYSIS OF THE CABLE-DRIVEN CONTINUUM ROBOT

Based on the segmented cable-driven scheme, the forward kinematic model of a CDCR can be formulated as the product of the kinematic models of the CDSs:

$$T_{0,n}(\alpha, \theta) = T_{0,1}(\alpha_1, \theta_1)\cdots T_{i-1,i}(\alpha_i, \theta_i)\cdots T_{n-1,n}(\alpha_n, \theta_n) \tag{13}$$

Given joint variables of all CDSs, the pose of the end platform for the CDCR described in the base frame can be uniquely determined according to the number and sequence of the CDSs.

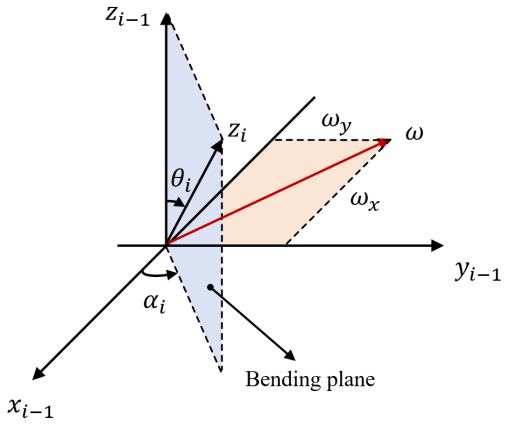

FIGURE 3. Rotation of the 2-DOF CDS.

C. COMPUTATION EXAMPLE

In order to illustrate the effectiveness of the proposed kinematics modeling method, a computation example is presented. As shown in Fig.6, a CDCR is composed by four CDSs and the height of each CDS is $L = 120\,\text{mm}$. The radius of the circle where the anchorage points are located is $r = 70\,\text{mm}$. Given the lengths of sixteen driving cables, the joints variables and the corresponding pose of the end platform described in the base frame can be computed. The computation results are presented in Table 1.

IV. TIP ERROR COMPENSATION

Although the forward kinematic model of the CDCR presented in Section III is greatly simplified, it is still not accurate due to the complex deflection of the flexible backbone and the influence of the machining error and assembly error introduced to the CDCR. Gaussian Process Regression (GPR) is employed to compensate the tip error of the CDCR based on the formulated kinematic model. It is worth to mention that GPR has been employed for the calibration of the industrial robots and demonstrates its effectiveness and robustness [18], [19].

A. GAUSSIAN PROCESS REGRESSION

GPR is a supervised learning method employed for data prediction, in which Gaussian Process (GP) is employed to describe the function distribution. GP is the combination of wilfully finite random variables with the joint Gaussian distribution, whose property is merely determined by the mean function and the covariance function [20]. Generally, the mean function of the GP model is transformed into zero through data preprocessing in order to simplify the learning process. Therefore, it just requires to train the tunable learning parameters of the covariance function during the learning process. Compared with other machine learning methods, GPR merely requires several learning parameters and a small amount of training data, which increases the computational efficiency of the learning process.

During the learning process, the training data set and the verification test data set are employed to update the GP model and evaluate the updated GP model, respectively. The learning process and the prediction process are presented as follows.

Given n sets of training data (x_i, y_i), $i = 1, 2, \ldots, n$, the corresponding outputs predicted by the GP model are assumed as the normal distribution:

$$y \sim N(0, K) \tag{14}$$

where $K \in \Re^{n\times n}$ is the covariance matrix of the GP model, and K_{ij} is the relevance measurement between x_i and x_j.

In (14), the square exponential covariance is employed as the covariance function for the GP model:

$$K_{ij} = K(x_i, x_j) = \sigma^2 \exp(\frac{1}{2}(x_i - x_j)^T \ell^{-2}(x_i - x_j)) \tag{15}$$

TABLE 1. Computation results for the forward kinematic analysis.

Cases	Driving cable lengths (mm)	Joint variables (rad)	Poses of the end platform
1	120,120,120,120 120,120,120,120 120,120,120,120 120,120,120,120	0,0 0,0 0,0 0,0	$\begin{bmatrix} 1 & 0 & 0 & 0 \\ 0 & 1 & 0 & 0 \\ 0 & 0 & 1 & 480 \\ 0 & 0 & 0 & 1 \end{bmatrix}$
2	118,123,124,115 124,115,118,121 110,117,125,123 124,105,112,128	0.9273, 0.0714 -2.3562,0.0606 -0.3805,0.1155 -2.0517,0.1856	$\begin{bmatrix} 0.9997 & 0.0125 & 0.0200 & 19.2070 \\ -0.0084 & 0.9814 & -0.1917 & -6.3962 \\ -0.0220 & 0.1914 & 0.9813 & 478.3811 \\ 0 & 0 & 0 & 1 \end{bmatrix}$
3	124,121,114,117 122,113,116,125 112,119,126,123 121,128,112,110	2.7611, 0.0769 -2.0344,0.0959 -0.2783,0.1040 2.0344,0.1439	$\begin{bmatrix} 0.9969 & -0.0028 & -0.0789 & -28.6431 \\ 0.0062 & 0.9991 & 0.0428 & -11.1228 \\ 0.0787 & -0.0432 & 0.9960 & 478.4405 \\ 0 & 0 & 0 & 1 \end{bmatrix}$
4	128,114,110,125 124,116,113,126 121,116,117,123 124,118,115,122	-2.5930, 0.1508 -2.4038,0.1062 2.0899,0.0576 -2.7234,0.0704	$\begin{bmatrix} 0.9555 & -0.0354 & -0.2928 & -85.4021 \\ -0.0325 & 0.9741 & -0.2237 & -64.3812 \\ 0.2931 & 0.2232 & 0.9296 & 465.2294 \\ 0 & 0 & 0 & 1 \end{bmatrix}$
5	125,110,112,127 114,118,127,124 114,115,125,123 123,127,117,114	-2.2236, 0.1530 -0.4324,0.1023 -0.6288,0.0972 2.0032,0.1023	$\begin{bmatrix} 0.9993 & -0.0107 & 0.0358 & 0.6157 \\ 0.0152 & 0.9917 & -0.1277 & -68.0789 \\ -0.0341 & 0.1282 & 0.9912 & 473.7015 \\ 0 & 0 & 0 & 1 \end{bmatrix}$

where σ and l are the tunable learning parameters of the covariance function, which can form a parameter set $\theta = \{\sigma^2, l^2\}$.

In order to solve the optimal solution of learning parameters, the maximum likelihood function of the hyper-parameter set $L(\theta) = -\log p(y \mid X, \theta)$ is employed for the training data, where $X = [x_1, \cdots, x_n]$. Through minimizing the maximum likelihood function $L(\theta)$, the optimal hyper-parameters can be obtained.

After training, it is required to verify the effectiveness of the GP model. Given a verification test point $(x_{\text{test}}, y_{\text{test}})$, the predicted output $y_{\text{test}}^{\text{gp}}$ based on the Bayesian inference can be determined by

$$y_{\text{test}}^{\text{gp}} | y \sim N(K_{\text{test}} K^{-1} y, K_{\text{tt}} K_{\text{test}} K^{-1} K_{\text{test}}^T) \tag{16}$$

where $K_{\text{test}} = K(X, x_{\text{test}}) = K(x_{\text{test}}, X)^T$ is the covariance matrix between x_{test} and the input matrix X, and $K_{\text{tt}} = K(x_{\text{test}}, x_{\text{test}})$ is the auto-covariance of x_{test}.

Through comparing the actual output y_{test} with the predicted output of the GP model $y_{\text{test}}^{\text{gp}}$, the effectiveness of the GP model for data prediction is certified.

B. COMPENSATION PROCESS

For the CDCR with four CDSs as shown in Fig.6, the input of the GP model is the joint variables from the first CDS to the forth CDS:

$$x = [\alpha_1, \theta_1, \alpha_2, \theta_2, \alpha_3, \theta_3, \alpha_4, \theta_4] \tag{17}$$

The actual output of the GP model is the initial tip error of the CDCR. According to the local POE formula [21], the tip error is given as

$$\varepsilon = \log(T_{0,n}^a (T_{0,n}^n)^{-1})^\vee \tag{18}$$

where $T_{0,n}^a$ represents the measured pose of the end platform with respect to the base frame of the CDCR, and $T_{0,n}^n$ represents the computed pose of the end platform with respect to the base frame calculated through (13). $\log(T)^\vee$ denotes the mapping from the kinematic transformation matrix $T \in SE(3)$ to a twist $\varepsilon \in \Re^{6\times 1}$. The flowchart of the learning process for the joint variables and the corresponding tip errors is given in Fig.4.

The updated GP model can be transformed into a matrix $T_{\text{gp}} \in SE(3)$ through the exponential mapping, which is used to compensate the nominal kinematic model:

$$T_{0,n}^c = T_{\text{gp}} T_{0,n}^n \tag{19}$$

To evaluate the effectiveness of the updated GP model, the residual tip error after compensation $d\varepsilon$ is calculated:

$$d\varepsilon = \log(T_{0,n}^a (T_{0,n}^c)^{-1})^\vee \tag{20}$$

According to the aforementioned tip error compensation method, the accuracy of the kinematic model is significantly improved, which increases the positioning accuracy of the CDCR.

V. EXPERIMENTAL SET-UP AND RESULTS

A. EXPERIMENTAL SET-UP

In order to validate the effectiveness of the proposed integrated accuracy enhancement method, experiments based on the actual testbed are conducted. An experimental testbed is built referring to Fig.5, which includes the prototype of the CDCR, the actuation devices, the Qualisys Track Manager (QTM) with six cameras and an Industrial Personal Computer (IPC).

As shown in Fig.6, the prototype of the CDCR is composed by four CDSs. The height of each CDS is 120 mm, which is

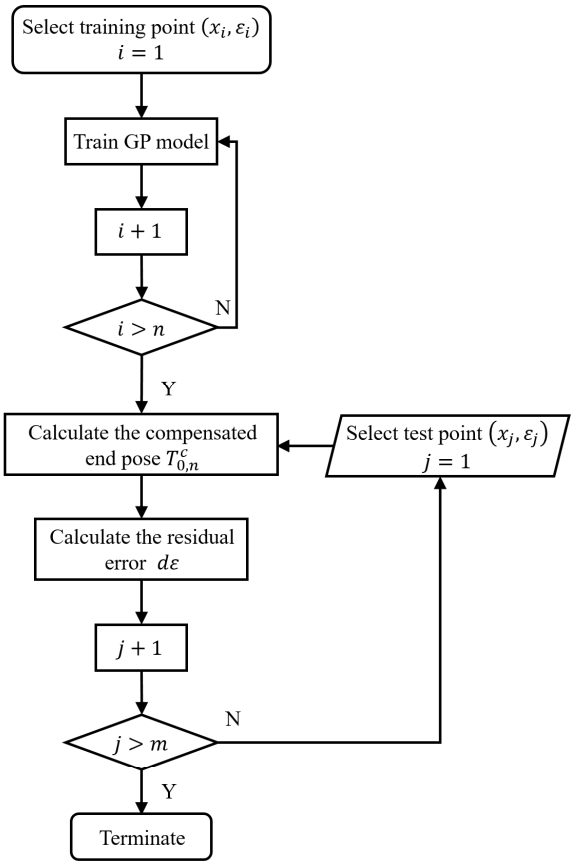

FIGURE 4. Flowchart of the learning process.

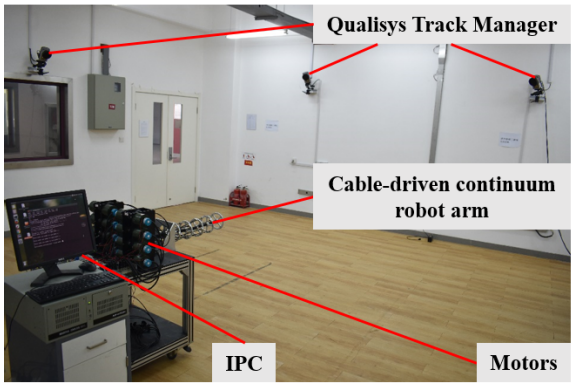

FIGURE 5. Experimental setup for the tip error compensation.

the length of the flexible backbone for the CDS. The radius of the circle where mounting points are located is 67 mm. The driving cables employ the steel wire rope whose diameter is 2 mm. In the CDCR prototype, each CDS has four driving cables and each driving cable is independently controlled by a motor-driven actuation device. As such, sixteen actuation devices are employed, which are mounted on the bench. The flexible backbone employs a wire braided hydraulic hose whose external diameter is 19 mm.

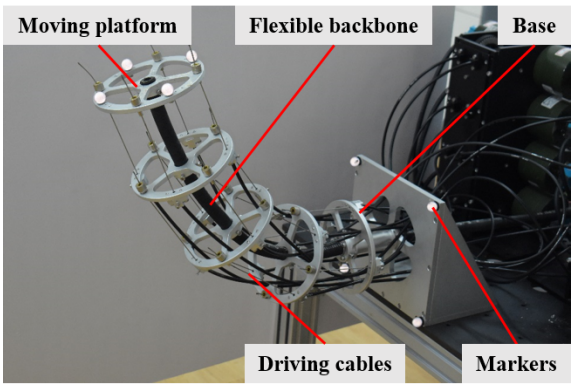

FIGURE 6. Prototype of the CDCR with four CDSs.

As the position repeatability of the CDCR is limited to a few millimetres, the QTM is employed as the position measurement, whose measurement accuracy is around 0.5 millimetre. In the experiment, four markers are fixed on the base and the other four markers are mounted on the end moving platform of the CDCR.

B. EXPERIMENTAL RESULTS

1) MEASURED DATA PROCESSING

During the experiment, QTM is employed to measure the position of each marker described in the camera coordinate system. The positions of the markers are used to build the coordinate systems of the base and the end moving platform with respect to the camera coordinate system, respectively. Through the transformation of coordinate systems, the actual pose of the end moving platform expressed in the base frame is given as

$$^{\text{end}}T_{\text{base}} = (^{\text{base}}T_{\text{camera}})^{-1} \cdot {}^{\text{end}}T_{\text{camera}} \tag{21}$$

where $^{\text{base}}T_{\text{camera}}$ represents the pose of the base platform described in camera coordinate system, and $^{\text{end}}T_{\text{camera}}$ represents the pose of the end platform described in camera coordinate system.

2) EXPERIMENTAL DATA PROCESSING

A total of 750 input-output pairs of data are employed in the experiment. The inputs are the joints variables which are randomly generated within the reachable workspace of the CDCR. The outputs are the corresponding initial tip errors of the CDCR calculated through (18). The inputs and the corresponding outputs make up a data set. 700 sets of training data are randomly selected from the data set as a training data set and the remaining 50 sets of data are selected as a verification test data set. The average initial tip error of the verification test data set before compensation is given in Table 2.

A number of training data are selected randomly from the training data set to learn the GP model according to the learning process presented in Section IV. The updated GP model is employed to modify the nominal kinematic model

TABLE 2. The average initial tip error.

	Position error (mm)	Orientation error (°)
Average initial error	53.1875	11.3961

TABLE 3. The residual tip errors with different numbers of training data.

Numbers of training data	Position errors (mm)	Orientation errors (°)
100	32.3689	10.0382
200	27.5285	7.8724
300	23.6977	6.9958
400	21.4668	6.4229
500	18.5873	5.9530
600	17.6589	5.6264
700	16.6392	5.5004

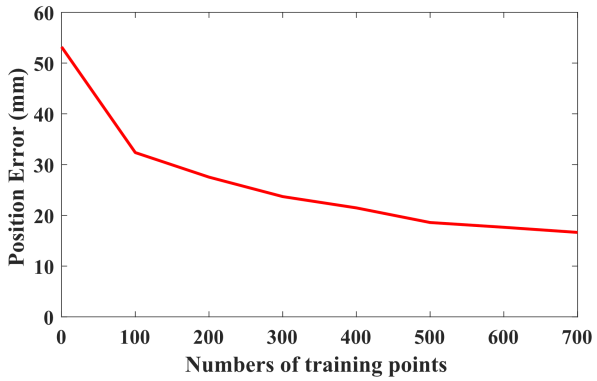

FIGURE 7. Experimental result about the relationship between the number of training data and residual position errors.

according to (19). The residual tip error of the verification test data is calculated through (20). Compared with the average initial tip error, the average residual error after compensation is significantly reduced.

Moreover, the relationship between the number of training data and the corresponding residual tip error has also been studied. As shown in Fig.7 and Fig.8, the average residual tip error gradually reduces with the increment of the number of training data. As shown in Table 3, the average residual tip error converges to 16.6 mm in position and 5.5° in orientation when the number of training data reaches to 700. The average residual tip error is reduced by 68.72% for position and 51.74% for orientation compared with the average initial tip error.

According to the experimental results, the proposed integrated accuracy enhancement method significantly reduces the tip errors of the CDCR, which includes not only the geometric errors but also the non-geometric errors resulting from the nonlinear characteristics of the driving cables, the parasitic deflection of the backbone, and etc. In this work, 300 to 500 sets of training data are enough to learn an accurate GP model, which also implies that the proposed data-driven GPR technique is computationally efficient. However, the compensated positioning accuracy is limited to 2 centimetres mainly due to the payload of the CDCR, which will be further studied in the future.

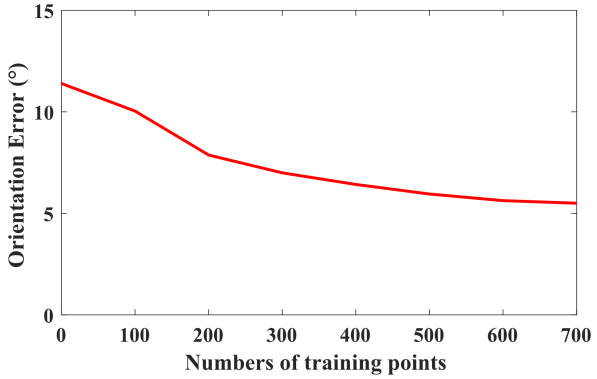

FIGURE 8. Experimental result about the relationship between the number of training data and residual orientation errors.

VI. CONCLUSION

In this paper, an integrated accuracy enhancement method is proposed to improve the positioning accuracy of the cable-driven continuum robot with a flexible backbone. The proposed method is based on both the kinematic model and the data-driven Gaussian Process Regression (GPR) technique. A two-parameter POE formula is employed to derive the analytic kinematic model of the CDCR, while GPR is proposed to compensate its tip errors. The integrated accuracy enhancement method compensates not only the geometric errors but also the non-geometric errors of a CDCR. The tip error of the CDCR is greatly reduced according to the experiment results. During the experiment, it is found that the payload has a great influence on the positioning accuracy of the CDCR. In the future, the payload will be considered as one of the GP model inputs.

REFERENCES

[1] R. Buckingham, "Snake arm robots," *Ind. Robot, Int. J.*, vol. 29, no. 3, pp. 242–245, Jun. 2002.
[2] Z. Li and R. Du, "Design and analysis of a bio-inspired wire-driven multi-section flexible robot," *Int. J. Adv. Robot. Syst.*, vol. 10, no. 4, p. 209, Jan. 2013.
[3] X. Dong, D. Axinte, D. Palmer, S. Cobos, M. Raffles, A. Rabani, and J. Kell, "Development of a slender continuum robotic system for on-wing inspection/repair of gas turbine engines," *Robot. Comput.-Integr. Manuf.*, vol. 44, pp. 218–229, Apr. 2017.
[4] K. Xu, J. Zhao, and M. Fu, "Development of the SJTU unfoldable robotic system (SURS) for single port laparoscopy," *IEEE/ASME Trans. Mechatronics*, vol. 20, no. 5, pp. 2133–2145, Oct. 2015.
[5] R. J. Webster, J. M. Romano, and N. J. Cowan, "Mechanics of precurved-tube continuum robots," *IEEE Trans. Robot.*, vol. 25, no. 1, pp. 67–78, Feb. 2009.
[6] M. Cianchetti, A. Arienti, M. Follador, B. Mazzolai, P. Dario, and C. Laschi, "Design concept and validation of a robotic arm inspired by the octopus," *Mater. Sci. Eng. C*, vol. 31, no. 6, pp. 1230–1239, Aug. 2011.
[7] M. Manti, A. Pratesi, E. Falotico, M. Cianchetti, and C. Laschi, "Soft assistive robot for personal care of elderly people," in *Proc. 6th IEEE Int. Conf. Biomed. Robot. Biomechatronics (BioRob)*, Jun. 2016, pp. 833–838.
[8] J. S. Mehling, M. A. Diftler, M. Chu, and M. Valvo, "A minimally invasive tendril robot for in-space inspection," in *Proc. 1st IEEE/RAS-EMBS Int. Conf. Biomed. Robot. Biomechatronics (BioRob)*, Feb. 2006, pp. 690–695.
[9] M. W. Hannan and I. D. Walker, "Kinematics and the implementation of an Elephant's trunk manipulator and other continuum style robots," *J. Robot. Syst.*, vol. 20, no. 2, pp. 45–63, Feb. 2003.
[10] N. Simaan, R. Taylor, and P. Flint, "A dexterous system for laryngeal surgery," in *Proc. IEEE Int. Conf. Robot. Autom. (ICRA)*, 2004, vol. 1, no. 6, pp. 351–357.

[11] I. Gravagne and I. D. Walker, "Kinematics for constrained continuum robots using wavelet decomposition," in *Proc. Robot.*, Apr. 2012, pp. 292–298.
[12] M. Giorelli, F. Renda, M. Calisti, A. Arienti, G. Ferri, and C. Laschi, "Neural network and jacobian method for solving the inverse statics of a cable-driven soft arm with nonconstant curvature," *IEEE Trans. Robot.*, vol. 31, no. 4, pp. 823–834, Aug. 2015.
[13] W. Xu, J. Chen, H. Y. K. Lau, and H. Ren, "Data-driven methods towards learning the highly nonlinear inverse kinematics of tendon-driven surgical manipulators," *Int. J. Med. Robot. Comput. Assist. Surg.*, vol. 13, no. 3, p. e1774, Sep. 2016.
[14] R. Grassmann, V. Modes, and J. Burgner-Kahrs, "Learning the forward and inverse kinematics of a 6-DOF concentric tube continuum robot in SE(3)," in *Proc. IEEE/RSJ Int. Conf. Intell. Robots Syst. (IROS)*, Oct. 2018, pp. 5125–5132.
[15] Z. Zhang, G. Yang, S. H. Yeo, W. B. Lim, and S. K. Mustafa, "Design optimization of a cable-driven two-DOF joint module with a flexible backbone," in *Proc. IEEE/ASME Int. Conf. Adv. Intell. Mechatronics*, Jul. 2010, pp. 385–390.
[16] W. Shen, G. Yang, T. Zheng, Y. Wang, K. Yang, Z. Fang, and C. Zhang, "An integrated accuracy enhancement method for cable-driven flexible continuum robot," in *Proc. IEEE/ASME Int. Conf. Adv. Intell. Mechatronics (AIM)*, Jul. 2019, pp. 1121–1126.
[17] R. M. Murray, *A Mathematical Introduction to Robotic Manipulation*. Boca Raton, FL, USA: CRC Press, 1994.
[18] W. Jing, P. Y. Tao, G. Yang, and K. Shimada, "Calibration of industry robots with consideration of loading effects using product-of-exponential (POE) and Gaussian process (GP)," in *Proc. IEEE Int. Conf. Robot. Autom. (ICRA)*, May 2016, pp. 4380–4385.
[19] W. Jing, J. T. Zhou, F. Gao, Y. Liu, P. Y. Tao, and G. Yang, "A learning-based approach for error compensation of industrial manipulator with hybrid model," in *Proc. 15th Int. Conf. Control, Autom., Robot. Vis. (ICARCV)*, Nov. 2018, pp. 216–221.
[20] C. E. Rasmussen, "Gaussian processes in machine learning," in *Summer School on Machine Learning*. Berlin, Germany: Springer, 2003, pp. 63–71.
[21] I.-M. Chen, G. Yang, C. T. Tan, and S. H. Yeo, "Local POE model for robot kinematic calibration," *Mechanism Mach. Theory*, vol. 36, nos. 11–12, pp. 1215–1239, Nov. 2001.

WENJUN SHEN received the B.E. degree in mechanical design, manufacture, and automation from the China University of Geosciences, Wuhan, China, in 2017. She is currently pursuing the Ph.D. degree in mechanical manufacture and automation with the University of Chinese Academy of Sciences, Beijing, China.

Her research interests include mechanical design and the analysis of a cable-driven continuum robot with a flexible backbone.

GUILIN YANG (Member, IEEE) received the B.Eng. and M.Eng. degrees from Jilin University, China, in 1985 and 1988, respectively, and the Ph.D. degree from Nanyang Technological University, in 1999, all in mechanical engineering.

From 1998 to 2013, he was with the Singapore Institute of Manufacturing Technology (SIMTech), Singapore, as a Senior Scientist and the Manager of the Mechatronics Group. Since 2013, he has been with the Ningbo Institute of Materials Technology and Engineering, Chinese Academy of Sciences, where he is currently a Professor, the Deputy President of the institute, and the Director of the Zhejiang Key Laboratory of Robotics and Intelligent Manufacturing Equipment Technology. His research interests include a broad area of robotics and automation, such as precision electromagnetic actuators, compliant mechanisms, parallel-kinematics machines, cable-driven robots, modular robots, and robotic automation systems. He has published more than 280 technical articles in refereed journals and conference proceedings, authored three books, and filed 50 patents. He was a recipient of Research and Development 100 awards, in 2014.

TIANJIANG ZHENG received the B.S. degree in automation and the M.S. degree in control theory and control engineering from Shenyang Ligong university, Shenyang, China, in 2006 and 2009, respectively, and the Ph.D. degree in robotics, cognition, and interaction technology from Genova University.

From 2013 to 2015, he was Research Assistant with the Precision Drive and Advanced Robot Group, Ningbo Institute of Materials Technology and Engineering, Chinese Academy of Sciences, where he has been a Senior Engineer, since 2016. He has been published more than 20 articles and papers, and have applied more than ten patents. His research interests include the control of mobile robots, mobile manipulations, continuum manipulations, and parallel robots.

YI WANG received the B.E. degree in mechanical engineering from Southwest Jiaotong University, Chengdu, China, in 2015. He is currently pursuing the Ph.D. degree in mechanical engineering with the University of Chinese Academy of Sciences, Beijing, China, and the Ningbo Institute of Materials Technology and Engineering, Chinese Academy of Sciences, Ningbo, China.

His research interests include mechanical design, and the analysis and design of cable-driven manipulators.

KAISHENG YANG received the B.Eng. degree from the Zhejiang University of Technology, China, in 2008, and the M.Eng. degree from Zhejiang University, China, in 2011. He is currently pursuing the Ph.D. degree with the University of Chinese Academy of Sciences, China.

From 2011 to 2013, he worked as a Mechatronics Engineer in companies. Since 2013, he has been with the Zhejiang Marine Development Research Institute, China, as a Researcher in robotics and automation. His research interests are in cable-driven manipulators, bionic robots, and mechatronics systems.

ZAOJUN FANG received the B.E. degree from the University of Science and Technology Liaoning, Anshan, China, in 2005, and the M.E. and Ph.D. degrees from the Institute of Automation, Chinese Academy of Sciences, Beijing, China, in 2008 and 2011, respectively.

He is currently a Professor with the Zhejiang Key Laboratory of Robotics and Intelligent Manufacturing Equipment Technology, Ningbo Institute of Materials Technology and Engineering, Chinese Academy of Sciences, Ningbo, China. His current research interests include robot vision, robot control, and automation.